Nanoscale Res Lett (2009) 4:498–502
DOI 10.1007/s11671-009-9272-3

NANO EXPRESS

# Symmetry Properties of Single-Walled $BC_2N$ Nanotubes

**Hui Pan · Yuan Ping Feng · Jianyi Lin**

Received: 30 September 2008 / Accepted: 6 February 2009 / Published online: 24 February 2009


**Abstract** The symmetry properties of the single-walled $BC_2N$ nanotubes were investigated. All the $BC_2N$ nanotubes possess nonsymmorphic line groups. In contrast with the carbon and boron nitride nanotubes, armchair and zigzag $BC_2N$ nanotubes belong to different line groups, depending on the index n (even or odd) and the vector chosen. The number of Raman- active phonon modes is almost twice that of the infrared-active phonon modes for all kinds of $BC_2N$ nanotubes.

**Keywords** $BC_2N$ nanotubes · Symmetry · Group theory

## Introduction

Carbon nanotubes have been extensively studied because of their interesting physical properties and potential applications. Motivated by this success, scientists have been exploring nanotubes and nanostructures made of different materials. In particular, boron carbon nitride ($B_xC_yN_z$) nanotubes have been synthesized [1, 2]. Theoretical studies have also been carried out to investigate the electronic, optical and elastic properties of $BC_2N$ nanotubes using the first-principles and tight-binding methods, respectively [3–6].

Besides the elastic and electronic properties, theoretical and experimental research on phonon properties of $BC_2N$ nanotubes is also useful in understanding the properties of the nanotubes. For example, the electron–phonon interaction is expected to play crucial roles in normal and superconducting transition. Furthermore, symmetry properties of nanotubes have profound implications on their physical properties, such as photogalvanic effects in boron nitride nanotubes [7]. Studies on the symmetry properties of carbon nanotubes predicted the Raman- and infrared-active vibrations in the single-walled carbon nanotubes [8], which are consistent with the experimental data [9] and theoretical calculations [10]. A similar work was carried out by Alon on boron nitride nanotubes [11], and the results were later confirmed by first-principles calculations [12]. And the symmetry of $BC_2N$ nanotube was reported [13]. The purpose of this study is to extend the symmetry analysis to $BC_2N$ nanotubes and to determine their line groups. The vibrational spectra of $BC_2N$ nanotubes are predicted based on the symmetry. The number of Raman- and infrared (IR)-active vibrations of the $BC_2N$ nanotubes is determined accordingly.

## Structures of $BC_2N$ Nanotubes

Similar to carbon or boron nitride nanotubes [14, 15], a single-walled $BC_2N$ nanotube can be completely specified by the chiral vector which is given in terms of a pair of integers ($n$, $m$) [3]. However, compared to a carbon and boron nitride nanotubes, different $BC_2N$ nanotubes can be obtained by rolling up a $BC_2N$ sheet along different directions, as shown in Fig. 1a, because of the anisotropic

H. Pan · Y. P. Feng
Department of Physics, National University of Singapore, 2 Science Drive 2, 117542 Singapore, Singapore

H. Pan (✉)
Environmental Science Division, Oak Ridge National Laboratory, 37831 Oak Ridge, TN, USA
e-mail: panh1@ornl.gov

J. Lin
Institute of Chemical and Engineering Sciences, 1 Pesek Road, 627833 Jurong Island, Singapore

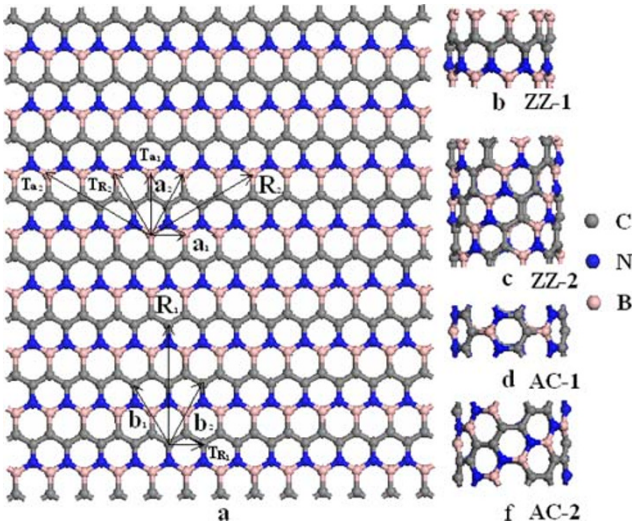


**Fig. 1** Atomic configuration of an isolated $BC_2N$ sheet. Primitive and translational vectors are indicated

geometry of the $BC_2N$ sheet. If we follow the notations for carbon nanotubes [14], at least two types of zigzag $BC_2N$ nanotubes and two types of armchair nanotubes can be obtained [6]. For convenience, we refer the two zigzag nanotubes obtained by rolling up the $BC_2N$ sheet along the $\mathbf{a}_1$ and the $\mathbf{a}_2$ directions as *ZZ*-1 and *ZZ*-2, respectively, and two armchair nanotubes obtained by rolling up the $BC_2N$ sheet along the $R_1$ and $R_2$ directions as AC-1 and AC-2, respectively. The corresponding transactional lattice vectors along the tube axes are $T_{a1}$, $T_{a2}$, $T_{R1}$, and $T_{R2}$, respectively, as shown in Fig. 1a. It is noted that $T_{a2}$ is parallel to $R_2$, $T_{R1}$ to $b_1$, and $T_{R2}$ to $a_2$. An example of each type of $BC_2N$ nanotubes is given in Fig. 1b–f.

## Symmetry of $BC_2N$ Nanotubes

We first consider the achiral carbon nanotubes with the rotation axis of order $n$, i.e., zigzag $(n, 0)$ or armchair $(n, n)$. The nonsymmorphic line-group [16] describing such achiral carbon nanotubes can be decomposed in the following way [17]:

$$G[n] = L_{T_z} \times D_{nh} \times [E \oplus S_{2n}] = L_{T_z} \times D_{nd} \times [E \oplus S_{2n}] \tag{1}$$

where $L_{T_z}$ is the 1D translation group with the primitive translation $T_z = |\mathbf{T_z}|$, and $\mathbf{E}$ is the identity operation. The screw axis $S_{2n} = (z \to z + T_z/2, \varphi \to \varphi + \pi/n)$ involves the smallest nonprimitive translation and rotation [11].

The corresponding $BC_2N$ sheet of the zigzag $(n, 0)$ $BC_2N$ nanotubes (*ZZ*-1) (Fig. 1b) is shown in Fig. 2. They have vertical symmetry planes as indicated by **g**. In this case, the $D_{nh}$ and $D_{nd}$ point groups reduce to $C_{nv}$ due to the

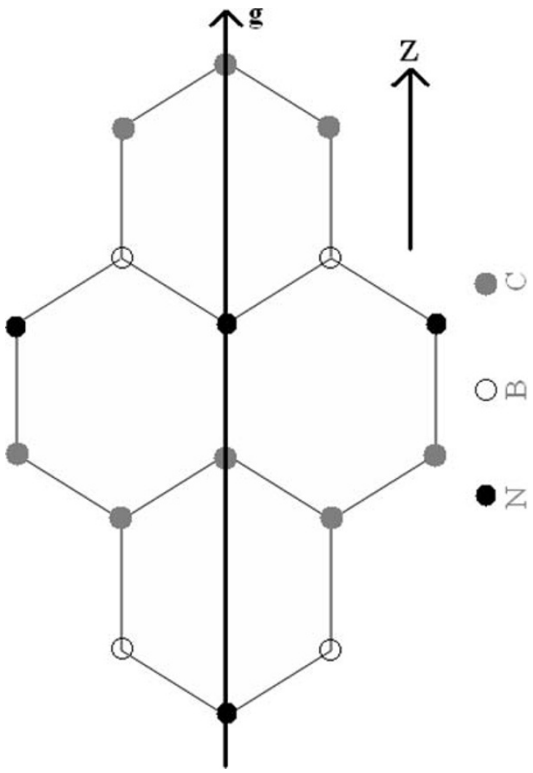


**Fig. 2** 2D projections of zigzag BC2N nanotubes (ZZ-1). **z** is a glide plane

lack of horizontal symmetry axis/plane, and $S_{2n}$ vanishes for the lack of the screw axis. Thus,

$$G^{zz-1}[n] = L_{T_z} \times C_{nv} \times E \tag{2}$$

The point group of the line group is readily obtained from Eq. 2,

$$G_0^{zz-1}[n] = C_{nv}. \tag{3}$$

To determine the symmetries at the Γ point of the 12 N ($N$ is the number of unit cells in the tube and $N = n$ for ZZ-1 $BC_2N$ nanotubes) of phonons in *ZZ*-1 $BC_2N$ nanotubes and the number of Raman- or IR-active modes, we have to associate them with the irreducible representations (irrep's) of $C_{nv}$. Here, two cases need to be considered.

Case 1

$n$ is odd (or $n = 2m + 1$, m is an integer)

The character table of $C_{(2m+1)v}$ possesses $m + 2$ irrep's [18], i.e.,

$$\Gamma_{C_{(2m+1)v}} = A_1 \oplus A_2 \oplus \sum_{j=1}^{m} E_j \tag{4}$$

The 12 N phonon modes transform according to the following irrep's:

$$\Gamma_{12N}^{ZZ-1} = \Gamma_o^{ZZ-1} \otimes \Gamma_v = 8A_1 \oplus 4A_2 \oplus \sum_{j=1}^{m} 12E_j \quad (5)$$

where

$$\Gamma_o^{ZZ-1} = 4A_1 \oplus \sum_{j=1}^{m} 4E_j (\mathrm{N} = \mathrm{n}) \quad (6)$$

stands for the reducible representation of the atom positions inside the unit cell. The prefactor of 4 in $\Gamma_o^{ZZ-1}$ reflects the four equivalent and disjoint sublattices made by the four atoms in the *ZZ*-1 $BC_2N$ nanotubes. $\Gamma_v = A_1 \oplus E_1$ is the vector representation. Of these modes, the ones that transform according to $\Gamma_t = A_1 \oplus E_1 \oplus E_2$ (the tensor representation) or $\Gamma_v$ are Raman- or IR-active, respectively. Out of the 12 N modes, four have vanishing frequencies [19], which transform as $\Gamma_v$ and $\Gamma_{R_z} = A_2$ corresponding to the three translational degrees of freedom giving rise to null vibrations of zero frequencies, and one rotational degree about the tube's own axis, respectively.

$$\Gamma_{Raman}^{ZZ-1} = 7A_1 \oplus 11E_1 \oplus 12E_2 \Rightarrow n_{Rman}^{ZZ-1} = 30 \quad (7)$$

$$\Gamma_{IR}^{ZZ-1} = 7A_1 \oplus 11E_1 \Rightarrow n_{Ir}^{ZZ-1} = 18 \quad (8)$$

Case 2

$n$ is even (or $n = 2m$, $m$ is an integer)

The character table of $C_{2mv}$ possesses $m + 3$ irrep's [18], i.e.,

$$\Gamma_{C_{(2m+1)v}} = A_1 \oplus A_2 \oplus B_1 \oplus B_2 \oplus \sum_{j=1}^{m-1} E_j \quad (9)$$

The 12 N phonon modes transform according to the following irrep's:

$$\Gamma_{12N}^{ZZ-1} = \Gamma_e^{ZZ-1} \otimes \Gamma_v = 8A_1 \oplus 4A_2 \oplus 8B_1 \oplus 4B_2 \oplus \sum_{j=1}^{m-1} 12E_j \quad (10)$$

where

$$\Gamma_e^{ZZ-1} = 4A_1 \oplus 4B_1 \oplus \sum_{j=1}^{m-1} 4E_j (N = n) \quad (11)$$

$\Gamma_v = A_1 \oplus E_1$is the vector representation. Of these modes, the ones that transform according to $\Gamma_t = A_1 \oplus E_1 \oplus E_2$ (the tensor representation) or $\Gamma_v$ are Raman- or IR-active, respectively. Out of the 12 N modes, four (which transform as $\Gamma_v$ and $\Gamma_{R_z} = A_2$) have vanishing frequencies [16].

$$\Gamma_{Raman}^{ZZ-1} = 7A_1 \oplus 11E_1 \oplus 12E_2 \Rightarrow n_{Rman}^{ZZ-1} = 30 \quad (12)$$

$$\Gamma_{IR}^{ZZ-1} = 7A_1 \oplus 11E_1 \Rightarrow n_{Ir}^{ZZ-1} = 18 \quad (13)$$

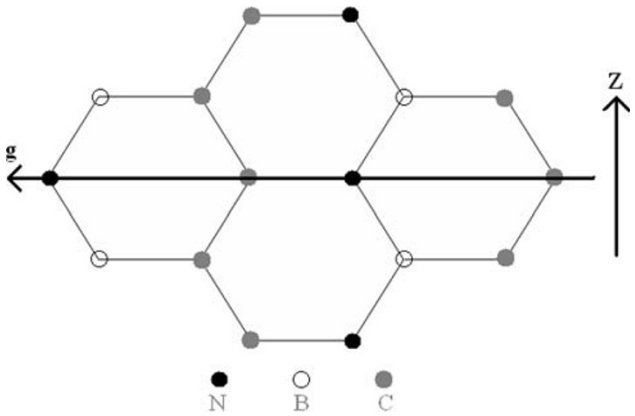


**Fig. 3** 2D projections of armchair BC2N nanotubes (AC-1). **z** is a glide plane

The numbers of Raman- and IR- active modes are 30 and 18, respectively, for *ZZ*-1 $BC_2N$ nanotubes irrespective $n$.

The armchair ($n$, $n$) $BC_2N$ nanotubes (AC-1) (Fig. 1d), corresponding to the $BC_2N$ sheet shown in Fig. 3, have horizontal planes as indicated by **g**. The $D_{nh}$ and $D_{nd}$ point groups reduce to $C_{nh}$ owing to the lack of $C_2$ axes and $S_{2n}$ vanishes for the lack of the screw axis.

$$G^{zz-1}[n] = L_{T_z} \times C_{nh} \times E \quad (14)$$

The point group of the line group is readily obtained from Eq. 2,

$$G_0^{zz-1}[n] = C_{nh} \quad (15)$$

To determine the symmetries (at the $\Gamma$ point) of the 12 N ($N = \mathrm{n}$) phonons in AC-1 $BC_2N$ nanotubes and the number of Raman- or IR-active modes, two cases need consideration, by associating them with the irrep's of $C_{nh}$.

Case 1

$n$ is odd ($n = 2\ \mathrm{m} + 1$)

The character table of $C_{(2m+1)h}$ possesses $4m + 2$ irrep's [18], i.e.,

$$\Gamma_{C_{(2m+1)v}} = A' \oplus A'' \oplus \sum_{j=1}^{m} \left\{ E_j'^{\pm} \oplus E_j''^{\pm} \right\} \quad (16)$$

The 12 N phonon modes transform according to the following irrep's:

$$\Gamma_{12N}^{AC-2} = \Gamma_o^{AC-2} \otimes \Gamma_v = 8A' \oplus 4A'' \oplus \sum_{j=1}^{m} \left\{ 4E_j' \oplus 8E_j'' \right\} \quad (17)$$

where

$$\Gamma_o^{AC-2} = 4A' \oplus \sum_{j=1,3,5,\ldots}^{m} 4E_j'^{\pm} \oplus \sum_{j=2,4,6,\ldots}^{m} 4E_j''^{\pm} \ (N = n) \quad (18)$$

and $\Gamma_v = A'' \oplus E_1'^{\pm}$ is the vector representation. Of these modes, the ones that transform according to $\Gamma_t = A' \oplus E_2'^{\pm} \oplus E_1''^{\pm}$ (the tensor representation) or $\Gamma_v$ are Raman- or IR-active, respectively. Out of the 12 N modes, four (which transform as $\Gamma_v$ and $\Gamma_{R_z} = A'$) have vanishing frequencies [19].

$$\Gamma_{Raman}^{AC-2} = 7A' \oplus 4E_2'^{\pm} \oplus 8E_1''^{\pm} \Rightarrow n_{Rman}^{AC-2} = 19 \quad (19)$$

$$\Gamma_{IR}^{AC-2} = 7A' \oplus 3E_1'^{\pm} \Rightarrow n_{Ir}^{ZZ-1} = 10 \quad (20)$$

Case 2

$n$ is even($n = 2m$)

The character table of $C_{2mh}$ possesses $4m$ irrep's [18], i.e.,

$$\Gamma_{C_{2mv}} = A_g \oplus B_g \oplus A_u \oplus B_u \oplus \sum_{j=1}^{m-1} \left\{ E_{jg}^{\pm} \oplus E_{jg}^{\pm} \right\} \quad (21)$$

The 12 N phonon modes transform according to the following irrep's:

$$\begin{aligned} \Gamma_{12N}^{AC-2} &= \Gamma_e^{AC-2} \otimes \Gamma_v \\ &= 8A_g \oplus 4B_g \oplus 4A_u \oplus 8B_u \oplus 4E_{1g}^{\pm} \oplus 8E_{2g}^{\pm} \oplus 4E_{3g}^{\pm} \\ &\quad \oplus \cdots \oplus \left[6 + 2(-1)^{m-1} E_{(m-1)g}^{\pm}\right] \oplus 8E_{1u}^{\pm} \oplus 4E_{2u}^{\pm} \\ &\quad \oplus 8E_{3u}^{\pm} \oplus \cdots \oplus [6 + 2(-1)^m] E_{(m-1)u}^{\pm} \end{aligned} \quad (22)$$

where

$$\Gamma_e^{AC-2} = 4A_g \oplus 4B_u \oplus \sum_{j=2,4,6,\ldots}^{m-1} 4E_{jg}^{\pm} \oplus \sum_{j=1,3,5,\ldots}^{m-1} 4E_{ju}^{\pm} (N = n) \quad (23)$$

$\Gamma_v = A_u \oplus E_{1u}^{\pm}$ is the vector representation. Of these modes, the ones that transform according to $\Gamma_t = A_g \oplus E_{1g}^{\pm} \oplus E_{2g}^{\pm}$ (the tensor representation) or $\Gamma_v$ are Raman- or IR-active, respectively. Out of the 12 N modes, four (which transform as $\Gamma_v$ and $\Gamma_{R_z} = A_g$) have vanishing frequencies [19].

$$\Gamma_{Raman}^{AC-2} = 7A_g \oplus 4E_{1g}^{\pm} \oplus 8E_{2g}^{\pm} \Rightarrow n_{Rman}^{AC-2} = 19 \quad (24)$$

$$\Gamma_{IR}^{AC-2} = 3A_u \oplus 7E_{1u}^{\pm} \Rightarrow n_{Ir}^{ZZ-1} = 10 \quad (25)$$

The numbers of Raman- and IR- active modes are 19 and 10, respectively, for AC-1 $BC_2N$ nanotubes in irrespective of n. The numbers of Raman- and IR- active phonon modes for $ZZ$-1 $BC_2N$ nanotubes are almost twice as for AC-1 $BC_2N$ nanotubes, which is similar to boron nitride nanotubes [11].

The nonsymmorphic line group describing the $(n', m')$-chiral carbon nanotubes can be decomposed as follows:

$$G[N] = L_{T_z} \times D_d \times \left[\sum_{j=0}^{N/d-1} S_{N/d}^j\right] = L_{t_z} \times D_1 \times \left[\sum_{j=0}^{N-1} S_N^j\right] \quad (26)$$

where $N = 2\left(n'^2 + m'^2 + n'm'\right)/d_R$; where $d_R$ is the greatest common divisor of $2n' + m'$ and $2m' + n'$; $d$ is the greatest common divisor of $n'$ and $m'$; $S_{N/d}$ and $S_N$ are the screw-axis operations with the orders of $N/d$ and $N$, respectively. The point group of the line group is obtained from Eq. 26,

$$G_0[N] = \sum_{j=0}^{N/d-1} C_{N/d}^j \times D_d = \sum_{j=0}^{N-1} C_N^j \times D_1 = D_N \quad (27)$$

where $C_{N/d} = (\phi \rightarrow \phi + 2d\pi/N)$ and $C_N = (\phi \rightarrow \phi + 2\pi/N)$ are the rotations embedded in $S_{N/d}$ and $S_N$, respectively.

For chiral $(n, m)$ $BC_2N$ nanotubes, the point group $D_N$ reduces to $C_N$ due for the lack of $C_2$ axes. Here, $N = \left(n'^2 + m'^2 + n'm'\right)/d_R$ $\left(n' = 2n, m' = m\right)$, where $d_R$ is the greatest common divisor of $2n' + m'$ and $2m' + n'$; $d$ is the greatest common divisor of $n'$ and $m'$. The $BC_2N$ sheets corresponding to $ZZ$-2 and $AC$-2 are shown in Fig. 4a and b, which are chiral in nature. The $\sigma_v$ and $\sigma_h$ vanish in Fig. 4a and b, respectively, for $ZZ$-2 and $AC$-2 $BC_2N$ nanotubes, $N = 4n$. The point group corresponding to the two models is expressed as:

$$G_0[N] = \sum_{j=0}^{N/d-1} C_{N/d}^j \times C_d = \sum_{j=0}^{N-1} C_N^j \times C_1 = C_N \quad (28)$$

The character table of $C_N$ has $N$ irrep's, i.e.,

$$\Gamma_{C_N}^{ch} = A \oplus B \oplus \sum_{j=1}^{N/2-1} E_j^{\pm} \quad (29)$$

The 12 N phonon modes transform according to the following irrep's:

$$\Gamma_{12N}^{ch} = \Gamma_a^{ch} \otimes \Gamma_v = 12A \oplus 12B \oplus \sum_{j=1}^{N/2-1} 12E_j^{\pm} \quad (30)$$

where $\Gamma_a^{ch} = 4\left(A \oplus B \oplus \sum_{j=1}^{N/2-1} E_j^{\pm}\right)$ and $\Gamma_v = A \oplus E_1^{\pm}$. Of these modes, the ones that transform according to $\Gamma_t = A \oplus E_1^{\pm} \oplus E_2^{\pm}$ and/or $\Gamma_v$ are Raman- and/or IR- active, respectively. Out of the 24 N modes, four (which transform as $\Gamma_v$ and $\Gamma_{R_z} = A$) have vanishing frequencies [19].

$$\Gamma_{Raman}^{ch} = 10A \oplus 11E_1^{\pm} \oplus 12E_2^{\pm} \Rightarrow n_{Rman}^{ch} = 33 \quad (31)$$

$$\Gamma_{IR}^{ch} = 10A \oplus 11E_1^{\pm} \Rightarrow n_{Ir}^{ZZ-1} = 21 \quad (32)$$

Experimentally, only several Raman/IR-active modes can be observed. The observable Raman-active modes are with the range of 0–2000 $cm^{-1}$. The $E_{2g}$ mode around 1580 $cm^{-1}$ is related to the stretching mode of C–C bond. The $E_{2g}$ mode around 1370 $cm^{-1}$ is attributed to B–N vibrational mode [20, 21]. The experimental Raman

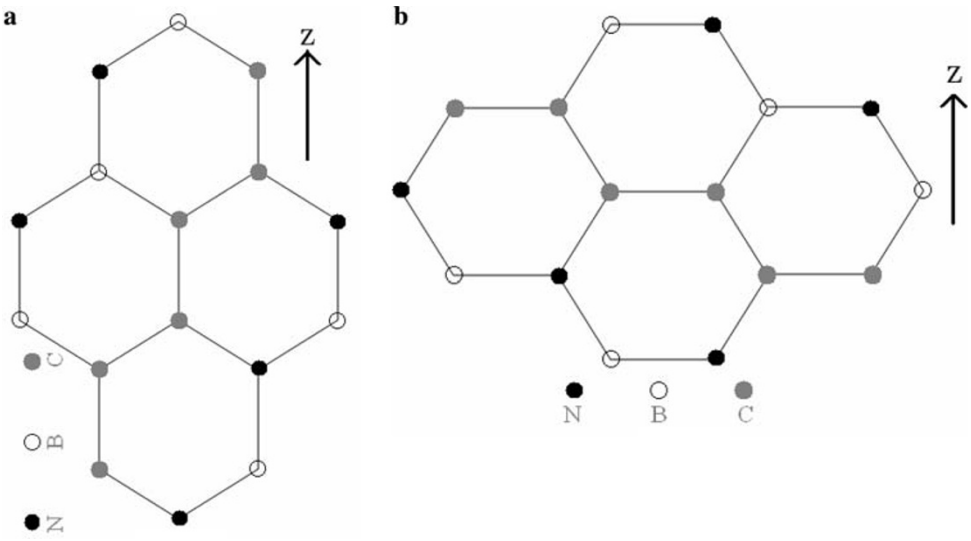


**Fig. 4** 2D projections of BC2N nanotubes **a** ZZ-2 and **b** AC-2. **z** is a glide plane

spectra between 100 and 300 $cm^{-1}$ should be attributed to $E_{1g}$ and $A_{1g}$ modes [22].

## Conclusions

In summary, the symmetry properties of $BC_2N$ nanotubes were discussed based on line group. All $BC_2N$ nanotubes possess nonsymmorphic line groups, just like carbon nanotubes [8] and boron nitride nanotubes [11]. Contrary to carbon and boron nitride nanotubes, armchair and zigzag $BC_2N$ nanotubes belong to different line groups, depending on the index n (even or odd) and the vector chosen. By utilizing the symmetries of the factor groups of the line groups, it was found that all *ZZ*-1 $BC_2N$ nanotubes have 30 Raman- and 18 IR- active phonon modes; all *AC*-1 $BC_2N$ nanotubes have 19 Raman- and 10 IR-active phonon modes; all *ZZ*-2, *AC*-2, and other chiral $BC_2N$ nanotubes have 33 Raman- and 21 IR-active phonon modes. It is noticed that the numbers of Raman- and IR- active phonon modes in *ZZ*-1 $BC_2N$ nanotubes are almost twice as in *AC*-1 $BC_2N$ nanotubes, but which is almost the same as those in chiral, *ZZ*-2, and *AC*-2 $BC_2N$ nanotubes. The situation in $BC_2N$ nanotubes is different from that in carbon or boron nitride nanotubes [8, 11].

## References

1. Z. Weng-Sieh, K. Cherrey, N.G. Chopra, X. Blase, Y. Miyamoto, A. Rubio, M.L. Cohen, S.G. Louie, A. Zettl, R. Gronsky, Phys. Rev. B **51**, 11–229 (1995)
2. K. Suenaga, C. Colliex, N. Demoncy, A. Loiseau, H. Pascard, F. Willaime, Science **278**, 653 (1997). doi:10.1126/science.278.5338.653
3. Y. Miyamoto, A. Rubio, M.L. Cohen, S.G. Louie, Phys. Rev. B **50**, 4976 (1994). doi:10.1103/PhysRevB.50.4976
4. E. Hernández, C. Goze, P. Bernier, A. Rubio, Phys. Rev. Lett. **80**, 4502 (1998). doi:10.1103/PhysRevLett.80.4502
5. H. Pan, Y.P. Feng, J.Y. Lin, Phys. Rev. B **74**, 045409 (2006). doi:10.1103/PhysRevB.74.045409
6. H. Pan, Y.P. Feng, J.Y. Lin, Phys. Rev. B **73**, 035420 (2006). doi:10.1103/PhysRevB.73.035420
7. P. Kral, E.J. Mele, D. Tomanek, Phys. Rev. Lett. **85**, 1512 (2000). doi:10.1103/PhysRevLett.85.1512
8. O.E. Alon, Phys. Rev. B **63**, 201403(R) (2001)
9. A.M. Rao, E. Richter, S. Bandow, B. Chase, P.C. Eklund, K.A. Williams, S. Fang, K.R. Subbaswamy, M. Menon, A. Thess, R.E. Smalley, G. Dresselhaus, M.S. Dresselhaus, Science **275**, 187 (1997). doi:10.1126/science.275.5297.187
10. L.H. Ye, B.G. Liu, D.S. Wang, R. Han, Phys. Rev. B **69**, 235409 (2004). doi:10.1103/PhysRevB.69.235409
11. O.E. Alon, Phys. Rev. B **64**, 153408 (2001). doi:10.1103/PhysRevB.64.153408
12. L. Wirtz, A. Rubio, R.A. delaConcha, A. Loiseau, Phys. Rev. B **68**, 045425 (2003). doi:10.1103/PhysRevB.68.045425
13. M. Damnjanovic, T. Vukovic, I. Milosevic, B. Nikolic, Acta Crystallogr. A **57**, 304 (2001). doi:10.1107/S0108767300018857
14. M.S. Dresselhaus, G. Dresslhaus, P.C. Eklund, *Science of Fullerenes and Carbon Nanotubes* (Acadamic Press, San Diego, 1996), p. 804
15. A. Rubio, J.L. Corkill, M.L. Cohen, Phys. Rev. B **49**, 5081 (1994). doi:10.1103/PhysRevB.49.5081
16. M. Damnjanovic, I. Milosevic, T. Vukovic, R. Sredanovic, Phys. Rev. B **60**, 2728 (1999). doi:10.1103/PhysRevB.60.2728
17. M. Damnjanovic, M. Vujicic, Phys. Rev. B **25**, 6987 (1982). doi:10.1103/PhysRevB.25.6987
18. D.C. Harris, M.D. Bertolucci, *Symmetry and Spectroscopy: An Introduction to Vibrational and Electronic Spectroscopy* (Dover, New York, 1989)
19. C.Y. Liang, S. Krimm, J. Chem. Phys. **25**, 543 (1956). doi:10.1063/1.1742962
20. J. Wu, W. Han, W. Walukiewicz, J.W. Ager III, W. Shan, E.E. Haller, A. Zettl, Nano Lett. **4**, 647 (2004)
21. C.Y. Zhi, X.D. Bai, E.G. Wang, Appl. Phys. Lett. **80**, 3590 (2002). doi:10.1063/1.1479207
22. R. Saito, T. Takeya, T. Kimura, G. Dresselhaus, M.S. Dresselhaus, Phys. Rev. B **57**, 4145 (1998). doi:10.1103/PhysRevB.57.4145